The past and the future of the GAINS spectrometer @ GELINA

Adina Olacel[1,*], *Catalin* Borcea[1], *Marian* Boromiza[1], *Philippe* Dessagne[2], *Greg* Henning[2], *Myroslav* Kavatsyuk[3], *Nasser* Kalantar-Nayestanaki[3], *Maëlle* Kerveno[2], *Alexandru* Negret[1], *Markus* Nyman[4], *Andreea* Oprea[5], *Carlos* Paradela[5], and *Arjan* Plompen[5]

[1]Horia Hulubei National Institute for Physics and Nuclear Engineering, Magurele, Romania
[2]CNRS, Universite de Strasbourg, IPHC, Strasbourg, France
[3]Energy and Sustainability Research Institute Groningen, University of Groningen, Groningen, The Netherlands
[4]University of Helsinki, Department of Chemistry, Helsinki, Finland
[5]European Commission - Joint Research Centre, Geel, Belgium

Abstract. GAINS (Gamma Array for Inelastic Neutron Scattering), currently installed at the GELINA (Geel Electron Linear Accelerator) neutron source of the EC-JRC (European Commission-Joint Research Centre), is one of the best instruments available worldwide for measuring high resolution, low uncertainty neutron inelastic cross-section data relevant for both fundamental research and nuclear physics applications (like Generation IV facilities). It features 12 HPGe detectors coupled with a ^{235}U fission chamber for neutron flux monitoring. The paper presents a short history of the GAINS development over the years and reviews some of the main experimental results together with plans for future experiments.

1 Introduction

Even after more than a century since its discovery by the Rutherford, Geiger and Marsden experiment [1], we still do not fully understand the atomic nucleus. Understanding the interaction between nucleons proved to be, and still is, a many-body problem which is very difficult to tackle both from an experimental and also theoretical point of view. If such detailed knowledge of nuclear structure would be available, it will allow in principle the calculation of all the interesting nuclear observables straight from first principles. Unfortunately, such goals are still out of our reach even though impressive progress has been made in the last decades. Nonetheless, all this effort translated into a plethora of nuclear models (both structure [2], [3] and reaction mechanisms [4]) which try to reproduce as best as possible some limited properties of the nucleus while neglecting the others, hence, losing generality and applicability. Nuclear physics has however an extensive list of applications, from the energy sector to space travel, which have stringent needs in terms of many nuclear observables like, as a typical example, cross sections. For the latter, the technological applications need continuous, extended, reliable and high precision cross-section data associated to many reaction channels [5]. Therefore, within this ecosystem, the nuclear data fill in a very important missing link: they bridge the gap between the stringent needs of nuclear applications and the fundamental nuclear physics research by providing many of the requested physical quantities. However, because most nuclear applications need very low uncertainty values and despite the progress already made, there is still much work to be done in the field. Arguments as the ones given above apply also to neutron-induced nuclear data, in particular, to the neutron inelastic channel. For example, such cross sections are very important in the design and construction of Generation IV nuclear facilities like fast reactors, accelerator driven systems, etc... These facilities will address most of the current issues of the nuclear energy sector such as safety, nuclear waste, fuel availability and many others. Because the inelastic scattering is the most important neutron energy loss mechanism inside a fast nuclear reactor, the community requires a huge improvement on the available neutron databases in terms of uncertainty and incident energy range. The most relevant cases get additional attention within the community with the latter identifying several target nuclei of special interest. These nuclei typically are listed on the High Priority Request List (HPRL) [6] managed by the IAEA, which consists of many reaction channels relevant for applications. Over the years, our group studied neutron-induced inelastic reactions on several isotopes using two HPGe detectors arrays: GAINS (Gamma Array for Inelastic Neutron Scattering) [7, 8] designed for light and medium mass nuclei (see Table 1) and GRAPhEME (GeRmanium array for Actinides PrEcise MEasurement) [24, 25] optimized for actinides (^{235,238}U [26, 27], ^{232}Th [28], $^{182-184,186,nat}$W [29]).

All of these experimental activities proved to be successful providing relevant data to the community. In this context, the present paper is dedicated to a short history of the GAINS spectrometer [7] operating at the GELINA (Geel Electron Linear Accelerator) neutron source [30] of the EC-JRC (European Commission - Joint Research Cen-

*e-mail: adina.olacel@nipne.ro

Table 1. The nuclei investigated up to now using GAINS. The references and some comments are given.

Nucleus	Comments	
^{52}Cr	[9]	2 HPGe detectors, analog DAQ
^{209}Bi	[10]	2 HPGe detectors, analog DAQ
^{208}Pb	[11]	4 HPGe detectors, analog DAQ
^{23}Na	[12]	8 HPGe detectors, digital DAQ
^{28}Si	[13]	8 HPGe detectors, digital DAQ
^{76}Ge	[14]	12 HPGe detectors, digital DAQ
^{56}Fe	[15]	8 HPGe detectors, digital DAQ
^{24}Mg	[16]	8 HPGe detectors, digital DAQ
^{206}Pb	[17]	4 HPGe detectors, digital DAQ
^{7}Li	[18]	12 HPGe detectors, digital DAQ
^{57}Fe	[19]	6 HPGe detectors, digital DAQ
$^{46-50}$Ti	[20]	12 HPGe detectors, digital DAQ
^{54}Fe	[21]	12 HPGe detectors, digital DAQ
^{16}O	[22]	12 HPGe detectors, digital DAQ
^{nat}Ni	[23]	12 HPGe detectors, digital DAQ
^{19}F	-	Data analysis in progress
^{40}Ca	-	Data analysis in progress
^{14}N	-	Data taking in progress

tre) to measure neutron inelastic cross section data. This setup uses γ-spectroscopy and neutron-time-of-flight techniques to extract the γ and neutron energies, respectively. We will shortly describe the GELINA facility and particular experiments performed by our group there, emphasizing interesting case studies, together with the main improvements done over the years to this setup. We will also mention important upgrades of the data acquisition system and future experiments our group plans to perform at GELINA.

2 The GAINS (Gamma Array for Inelastic neutron Scattering) spectrometer

GAINS is one of the several setups installed at the GELINA neutron time-of-flight facility of the EC-JRC Geel. GELINA is a pulsed, white neutron source currently operating at 400 Hz with a typical time resolution of 2 ns [30]. It consists of a high intensity electron accelerator (E_e=70-140 MeV) impinging on a depleted uranium target. The neutrons are generated via (γ, n) and (γ, f) reactions in the uranium target and travel along flight paths with different lengths (8 to 400 m) up to the cabins where the measurements take place.

Even though the HPGe-detectors-based setup used by our group at GELINA received its name (GAINS) only around 2008, its mission actually started in 2000 when two detectors, a ^{235}U fission chamber and conventional electronics were used at a 200 m distance from the neutron source to measure for the first time $(n, n'\gamma)$ cross sections at this facility. Over the years, GAINS was upgraded gradually to 4, 8 and finally 12 detectors. Also, the conventional data acquisition was replaced by a digital acquisition (DC440 Acqiris digitisers) after an extensive investigation and comparison of the two systems. This led to increasing

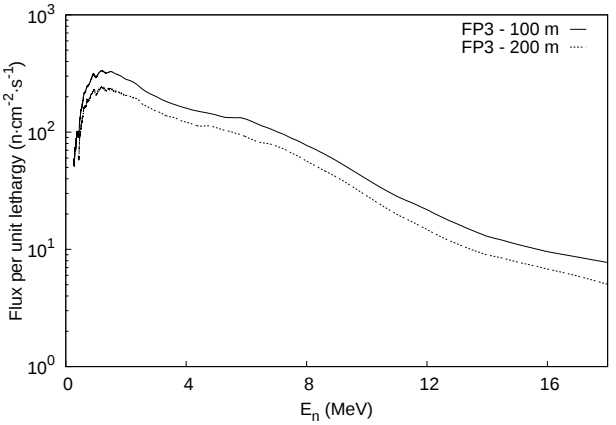

Figure 1. The neutron flux at the sample position in the 100-m and 200-m measurement cabins located on FP 3 of GELINA. Picture taken from Ref [21].

the γ-ray detection efficiency by 15% at 1.4 MeV and up to 300% at 350 keV [31] when switching from conventional to digital acquisition. In 2017, GAINS was moved to the 100-m measurement cabin in order to increase the neutron flux (see Fig. 1). Table 1 lists all the nuclei investigated over the years by our group together with the number of the detectors and the acquisition system used in each of these experiments.

Nowadays, GAINS is an array with 12 large volume HPGe detectors running on flight path 3 at 100 m from the neutron source (see Fig. 2). Here, the beam is collimated to a diameter of 61 mm while the 100-m flight path allows for a good neutron energy resolution: 3 keV at 1 MeV and 80 keV at 10 MeV. The detectors are placed at backward angles (110°, 125° and 150°) with respect to the neuron beam direction mainly to decrease as much as possible the effects of the γ-flash photons Compton-scattered by the sample. The detectors have a γ energy resolution of around 2.5 keV (for the 1332 keV peak of ^{60}Co) and a 100% relative efficiency. The acquisition is digital and consists of DC440 ACQIRIS digitisers having 12 bits amplitude resolution and a sampling frequency of 420 Msamples/s. Each digitiser has two inputs and a common trigger for two detectors. The data collected by the digitizers are transferred to the PC where an online processing is performed to determine the time and amplitude information for each detected event [32]. Currently, the collaboration is working on an upgrade of the data acquisition system. These activities were initiated by University of Groningen. Several possibilities are investigated but, most likely, the new system will be based on STRUCK SIS3316-250-14 SADC cards with 16 channels having a sampling frequency of 250 Msamples/s and 14 bits amplitude resolution [33]. These digitisers will also have a GBE readout and will be triggered internally using an external gate. Having a single digitizer module for all detectors is obviously advantageous as this, together with the bigger neutron flux at 100 m as compared to 200 m, could allow us to also perform coincidence measurements without the need for synchronizing different digitizer cards.

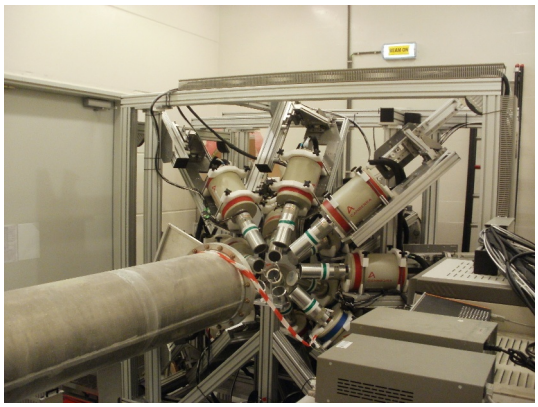

Figure 2. GAINS spectrometer operating on flight path 3 at 100 m from the GELINA neutron source.

We will keep, however, the neutron beam monitoring based on a ^{235}U fission chamber unchanged, given its proven reliability over the years, its relative simplicity to operate and the fact that ^{235}U(n, f) cross section [34] is a very well-known standard. The fission chamber is located around 1.7 m upstream the germanium array and it has a typical efficiency around 85% after several corrections are applied. The latter refer to polarization effects and corrections for the fraction of fission fragments that stop inside the ^{235}U deposits of the fission chamber or are below the alpha-FF discrimination threshold (see Ref. [35] for details).

3 The data analysis procedure

The data analysis procedure for our experiments at GELINA is well described in Refs. [36] and can be divided in three main steps:

- analysing the data collected by the HPGe detectors to extract the γ yields for all transitions,
- analysing the data collected by the fission chamber to gain information about the incident neutron flux (the fission-chamber yield)
- several corrections associated to these quantities: detector and fission chamber efficiencies, neutron multiple scattering, gamma-ray attenuation, etc.

We employ the digital trapezoid and constant fraction discriminator algorithms [31] to analyse the raw data and to determine time-amplitude list files for all the events of interest collected by the detectors. Because a typical experiment consists of months of data taking, this raises the issue of adding the statistics from several runs. We do this using in-house software which takes all list files and constructs, for each detector, a time-amplitude matrix that spans over the entire measurement campaign. Finally, we project this matrix on the time and amplitude axes to get the time and γ-ray spectra, respectively. We use the time information offered by the time spectra for incident neutron energy calibrations while the amplitude spectra are used to identify and integrate, with proper background subtraction, the γ peaks of all transitions of interest coming from the inelastic channel. This allows us to extract the γ yield as a function of neutron time of flight. This quantity needs then to be corrected for HPGe detector efficiency and neutron multiple scattering and beam attenuation inside the sample and on the surrounding materials.

To normalize the γ yields and gain information about the incident neutron flux, we have to analyze the data collected by the fission chamber. Similarly to the HPGe detectors, the raw data is sorted in a time-amplitude matrix which is then projected to get the time and amplitude spectra produced in the fission chamber. By separating the α-radioactivity and neutron-induced-fission regions in the amplitude spectra, we determine the fission chamber yield. This is then corrected for fission chamber efficiency, polarisation effects and for the fraction of fission fragments that are stopped in the ^{235}U deposits [35].

Having all these quantities, we can then calculate the differential γ-production cross sections at 110°, 125° and 150° for all the observed transitions using the formula:

$$\frac{d\sigma_j}{d\Omega}(\theta_i, E_n) = \frac{1}{4\pi} \cdot \frac{Y_j(E_n)}{Y_{FC}(E_n)} \cdot \frac{\varepsilon_{FC}}{\varepsilon_j(E_\gamma)} \cdot \frac{\rho_U}{\rho_s} \cdot \frac{A_s}{A_U} \cdot \frac{\sigma_U(E_n)}{c_{ms}(E_n)} \quad (1)$$

where θ_i is the detection angle, E_n is the incident neutron energy, E_γ is the γ energy, Y_j is the number of counts measured by the detector j for a given γ line, Y_{FC} is the fission chamber yield, ε_{FC} is the fission-chamber efficiency, $\varepsilon_j(E_\gamma)$ is the photopeak efficiency of the detector j, $\sigma_U(E_n)$ is the ^{235}U(n, f) cross section [34], ρ_U is the areal density of the uranium deposits from the fission chamber, A_U and A_s are the ^{235}U and sample atomic masses, ρ_s is the areal density of the sample and c_{ms} is the neutron multiple scattering correction factor. The differential cross section can be interpreted as the probability for γ emission at 110°, 125° or 150°.

Making use of known symmetries of the γ-emitting system, we can use the Gaussian Quadrature Method to calculate angle-integrated cross sections using the expression:

$$\sigma(E_n) = 4\pi[w_{110^\circ} \frac{d\sigma}{d\Omega}(110^\circ, E_n) + w_{150^\circ} \frac{d\sigma}{d\Omega}(150^\circ, E_n)] \quad (2)$$

where $\frac{d\sigma}{d\Omega}(110^\circ, E_n)$ and $\frac{d\sigma}{d\Omega}(150^\circ, E_n)$ are the above differential cross sections at 110° and 150°, respectively. The normalisation coefficients $w_{110^\circ} = 0.65214$ and $w_{150^\circ} = 0.34786$ are calculated by solving the system of equations resulting from a series expansion of the differential cross section in the Legendre polynomials basis as described in Refs. [31, 36, 37].

4 Selected results

This section highlights some particular results obtained by our group over the years using the GAINS spectrometer at the GELINA neutron source of EC-JRC Geel.

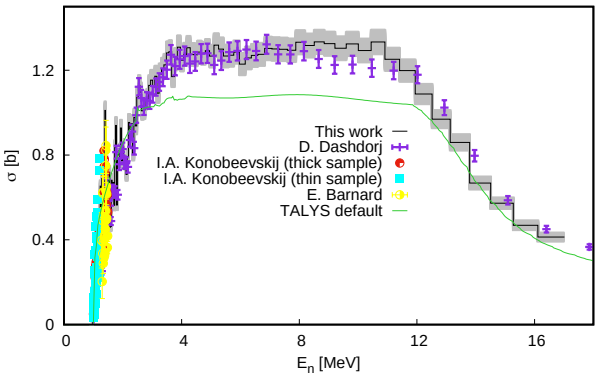

Figure 3. The γ production cross section of the first transition in ^{48}Ti in comparison with previous experimental results and with TALYS 1.8 theoretical calculations.

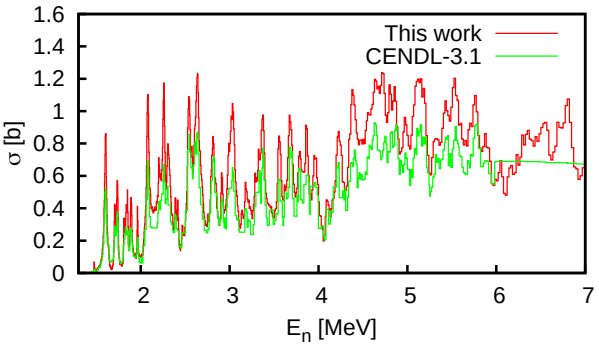

Figure 4. The neutron total inelastic cross section on ^{24}Mg, highlighting the 0-7 MeV region, in comparison with the CENDL-3.1 evaluation [42]. Picture taken from Ref. [16].

Table 2. Theoretical (ρ_t) versus experimental level densities (ρ_c) obtained in the ^{24}Mg$(n,n'\gamma)^{24}$Mg measurement.

E$_n$ range (MeV)	E*(^{25}Mg) (MeV)	ρ_t (MeV^{-1})	ρ_c (MeV^{-1})
1.73 – 2.78	2.26	19	18
2.78 – 3.82	3.30	36	18
3.82 – 4.87	4.34	53	10

The main transition in ^{48}Ti: a candidate for a γ-ray reference cross section for neutron-induced reactions

The main motivation for measuring the neutron-induced inelastic channel on several stable isotopes of titanium (we used a ^{nat}Ti target) relates to nuclear data needs for structural materials in nuclear reactors. However, in this case an additional motivation came from the ongoing effort of the nuclear data community to establish a γ-ray reference cross section for neutron-induced reactions. Several candidates are under consideration. The main transition in ^{48}Ti, at E_γ = 983.5 keV [38], is one such candidate due to its several advantages: i) ^{48}Ti is the most abundant isotope of titanium and has good mechanical and corrosion resistance (easy target production) and ii) the main transition has a relatively large cross section and an extended plateau region at around 1200 mb (see Fig. 3). The same figure also displays the TALYS theoretical calculation [39] for this transition using the default settings of the code. One can see that, even though the theoretical curve describes very well the threshold and high energy ranges, it greatly underestimates the plateau region by 200 mb. This is also the case for the other transitions in ^{48}Ti [20] indicating a poor quality neutron optical-model potential for this target nucleus. Therefore, when also considering the very good agreement with previously reported data for the 983.5-keV transition (see Fig. 3), the third motivation for measuring titanium concerned reaction mechanisms: providing very reliable and low uncertainty cross sections to constrain and improve reaction models.

Measuring individual resonances in the ^{25}Mg compound nucleus

The neutron inelastic channel on the even-even and relatively low level density nucleus ^{24}Mg was studied at the 200-m measurement cabin of GELINA [16]. This long flight path translated into a very good incident energy resolution, around 1 keV at 1 MeV and 35 keV at 10 MeV, and into more than 2500 cross section points for the most intense transitions. Such a detailed excitation function gave rise to the following question: are the resonances we observe individual (resolved) states in the compound nucleus or are they only overlapping of such states (Ericson fluctuations)? To answer this question, we performed some simple estimates of the level density in ^{25}Mg as a function of incident (and excitation) energy. We first calculated, using the TALYS reaction code, all the angular momentum and parity values populated in the compound nucleus. These values where then used as input quantities for a phenomenological formula - based on the Back-Shifted Fermi Gas model [39] and also on systematics for this mass region [40, 41] - to calculate theoretical level density values (ρ_t). The extracted results were compared with the values (ρ_c) obtained by a simple counting of the resonances we see in Fig 4 for the total inelastic cross section on ^{24}Mg.

Table 2 shows the results of this comparison for the ^{25}Mg compound nucleus. One can see that, at least in the neutron energy range 1.73-2.78 MeV, we are indeed able to separate individual states in the compound nucleus whereas above this incident energy we can only observe overlapping of such states. More details on this investigation and the ^{24}Mg$(n,n'\gamma)$ experiment are given in Ref. [16].

Inferring the neutron inelastic channel from proton-induced cross sections

This section highlights the results of our group's ongoing study aiming to relate the neutron and proton inelastic channels. If one would be able to infer neutron inelastic cross sections from an easier-to-measure charged particles reaction, this would open the possibility for experi-

ments on many very low abundance and/or high radioactivity isotopes due to the very high charged particles beam intensity that can be reached (typically orders of magnitude larger than the neutron beam intensity provided by GELINA). This would translate into a much better signal-to-background ratio thus allowing the γ-production cross section measurements for very weak transitions. In addition to this, a close comparison of neutron and proton reactions could yield new findings in respect to the reaction mechanism presently used to model these reactions and, in particular, can help better understand the role played by the isospin-dependent terms [43, 44] of the nucleon-target optical model potential.

We started this study in 2013 (see Ref. [45]) with an idea inspired by the surrogate reactions method [46–53]. In Ref. [45] we aimed to extract neutron inelastic cross sections on ^{28}Si from those obtained in an α-induced reaction: ^{28}Si$(n,n'\gamma)^{28}$Si versus ^{25}Mg$(\alpha,n\gamma)^{28}$Si. The two reactions proceed through the same compound nucleus (^{29}Si*) and have identical exit channels. In accordance with the Bohr hypothesis for compound nucleus reactions [54], this should generate similar γ-production cross sections in the two cases. Ref. [45] concludes, however, that a direct attempt to obtain neutron inelastic cross sections from the (α, n) reaction results in errors larger than 80-100%. This is explained by the relatively large difference in angular momentum populated in the compound nucleus by the two projectiles and by the different ground state spin of the two targets: 0^+ (^{28}Si) and $5/2^+$ (^{25}Mg) [45]. Moreover, in our subsequent study on ^{16}O and ^{28}Si [22], we discuss why a surrogate-type approach aiming to relate the neutron and proton inelastic channels yields very limited results. This is due to the fact that in this case the Weisskopf-Ewing approximation [55], which is crucial within the surrogate approach, does not hold when applied to the inelastic channel because of the relatively low excitation energy of states populated by the neutron and proton projectiles.

With this in mind, in Refs. [22, 23], we undertook a different approach to this problem. In order to minimize the differences generated by the nucleon-target optical model potential, we choose a proton-induced reaction on the same target. We measure the proton-induced inelastic cross sections at the 9 MV Tandem Accelerator of the Horia Hulubei National Institute for Physics and Nuclear Engineering, Magurele-Bucharest, Romania (details on the experimental setup we use in these experiments can be found in Ref. [22, 37]).

References [22, 23] show that, if the Coulomb barrier is removed in the incoming channel, the neutron and proton reactions behave very similarly (at least at the optical model stage of the calculations). In particular, the two projectiles populate practically identical angular momenta and parities in the compound nucleus while generating very similar transmission coefficients, direct contributions, compound elastic and reaction cross sections (see Figs. 9, 10 and 11 of Ref. [23]).

Exploiting all these similarities, we obtained a procedure - involving also theoretical input - able to relate the

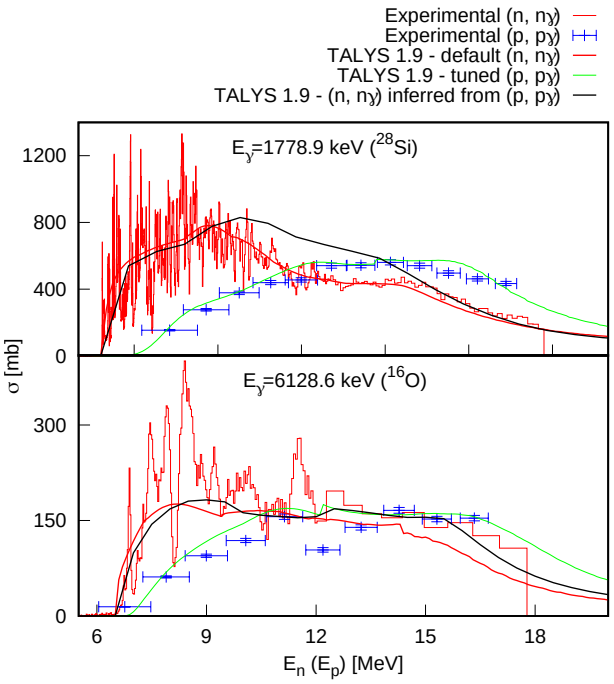

Figure 5. The results, given by the "TALYS 1.9 - $(n, n\gamma)$ inferred from $(p, p\gamma)$" curves, of our study aiming to relate the neutron and proton inelastic channels on ^{28}Si and ^{16}O (see Ref. [22] for full details).

neutron and proton inelastic channels with reasonable precision. It mainly consists of four steps:

- measure the proton-induced inelastic channel,
- model these cross sections as good as possible, using state-of-the-art reaction codes like TALYS 1.9 [39], and extract a tuned optical model after fixing its proton parameters using the constraints offered by experimental data,
- infer a neutron optical model potential on the same target nucleus by removing the Coulomb term and inverting the sign of the Lane term [43, 44] of the tuned proton potential,
- use the neutron-inferred potential to calculate neutron inelastic cross sections and compare the results with the experimental data measured at GELINA.

Figures 5,6 display the results we obtained using this approach for the main transition in ^{16}O, ^{28}Si and ^{58}Ni (see Refs. [22, 23] for the other transitions). In general, we are able to infer a neutron potential that describes a little better the neutron experimental data, as compared to the neutron default potential implemented in TALYS 1.9. Unfortunately, this is not the case for ^{28}Si where strong electromagnetic effects in the outgoing channels are clearly seen. With these reservations, the n-inferred cross sections show both the Lane-consistency of the nucleon optical model potential employed by reaction codes like TALYS and also that the isospin symmetry can be used, to a certain extent, to relate the neutron and proton inelastic channels. However, the improvement is only marginal and we refer the interested reader to Section V of Refs. [22, 23] for a detailed discus-

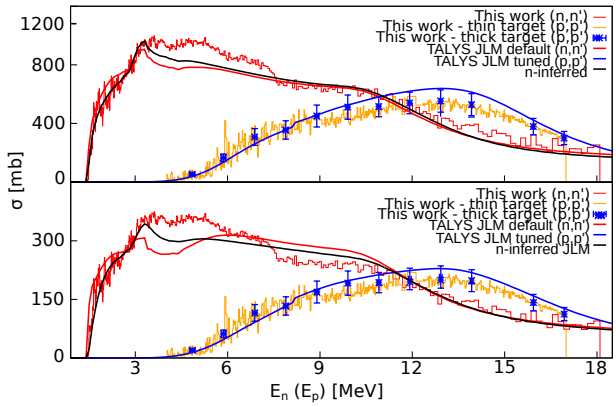

Figure 6. The results, given by the "n-inferred" curves, of our study aiming to relate the neutron and proton inelastic channels on ^{58}Ni (see Ref. [23] for full details).

sion of the observed discrepancies and possible ways to mitigate the main issues of our calculations, as currently implemented.

5 Conclusions

This paper gives a short history of the GAINS spectrometer currently installed in the 100-m measurement cabin on FP3 of the GELINA neutron source of the EC-JRC, Geel, Belgium. We present the main upgrades performed over the years to this setup together with some selected experimental results on ^{16}O, ^{24}Mg, ^{28}Si and ^{48}Ti. As for future planned experiments at GAINS we note:

- ^{14}N and ^{35,37}Cl - part of the Work Package 2 (New nuclear data measurements for energy and non-energy applications) Task 2.3 (Neutron elastic and inelastic scattering and neutron multiplication cross sections) within the Grant Agreement No. 847552 - SANDA (Supplying Accurate Nuclear Data for energy and non-energy Applications) european project and
- ^{56}Fe - this is a second measurement of our group on this isotope and it is motivated by the issues rose by the community, see Ref. [56] for details.

Acknowledgement

This work was supported by the European Commission's Seventh Framework Programme Fission-2013-CHANDA (Project No. 605203) and by the Romanian Ministry of Research, Innovation and Digitalization, CNCS-UEFISCDI, under contracts PN-III-P4-PCE-2021-0490 and PN 23 21 01 02. This project has also received funding from the Euratom research and training program 2014–2018 under Grant No. 847552 (SANDA). We would also like to thank all the people involved during the years to the development and upgrade of GAINS and the GELINA operators for their help and support during all the measurements.

References

[1] E. Rutherford, The London, Edinburgh, and Dublin Philosophical Magazine and Journal of Science, 21:125, 669-688, DOI: 10.1080/14786440508637080 (1911).
[2] P. Ring, P. Schuck, The nuclear many-body problem, Springer-Verlag, Berlin, Germany, 1980.
[3] K. Heyde, Basic ideas and concepts in nuclear physics:An Introductory Approach, Institute Of Physics Publishing, Bristol and Philadelphia, USA, 1999.
[4] G. R. Satchler, Introduction to nuclear reactions, Macmillan Education LTD, Oak Ridge, Tennessee, USA, 1990.
[5] United States Regulatory Commission, Nuclear Data Assessment for Advanced Reactors, Oak Ridge, Tennessee, USA, 2022 https://www.nrc.gov/docs/ML2206/ML22063A060.pdf.
[6] https://www.oecd-nea.org/jcms/c_12806/the-nea-high-priority-request-list-hprl-for-nuclear-data.
[7] D. Deleanu, C. Borcea, Ph. Dessagne, M. Kerveno, A. Negret, A.J.M. Plompen, J.C. Thiry, Nucl. Instrum. Methods Phys. Res. 624, 130 (2010).
[8] A. Negret et al., in Proceedings of the 2019 International Conference on Nuclear Data for Science and Technology (ND2019, Beijing, China, EPJ Web of Conferences, 239, 01005 (2020).
[9] L.C. Mihailescu, C. Borcea, A.J. Koning, A.J.M. Plompen, Nucl. Phys. A 786, 1 (2007).
[10] L.C. Mihailescu, C. Borcea, A.J. Koning, A. Pavlik, A.J.M. Plompen, Nucl. Phys. A 799, 1 (2008).
[11] L.C. Mihailescu, et al., Nucl. Phys. A 811, 1 (2008).
[12] C. Rouki, et al., Nucl. Instrum. Phys. Res. A 672, 82 (2012).
[13] A. Negret, et al., Phys. Rev. C 88, 034604 (2013).
[14] C. Rouki, A.R. Domula, J.C. Drohe, A.J. Koning, A.J.M. Plompen, K. Zuber, Phys. Rev. C 88, 054613 (2013).
[15] A. Negret, C. Borcea, Ph. Dessagne, M. Kerveno, A. Olacel, A. J. M. Plompen, and M. Stanoiu, Phys. Rev. C 90, 034602 (2014).
[16] A. Olacel, C. Borcea, P. Dessagne, M. Kerveno, A. Negret, A.J.M. Plompen, Phys. Rev. C 90, 034603 (2014).
[17] A. Negret, et al., Phys. Rev. C 91, 064618 (2015).
[18] M. Nyman, F. Belloni, D. Ichinkhorloo, E. Pirovano, A. J. M. Plompen, and C. Rouki, Phys. Rev. C 93, 024610 (2016).
[19] A. Negret, M. Sin, C. Borcea, R. Capote, Ph. Dessagne, M. Kerveno, N. Nankov, A. Olacel, A.J.M. Plompen, and C. Rouki, Phys. Rev. C 96, 024620 (2017).
[20] A. Olacel, et al., Phys. Rev. C 96, 014621 (2017).
[21] A. Olacel, et al., Eur. Phys. J. A 54:183 (2018).
[22] M. Boromiza, et al., Phys. Rev. C 101(2), 024604 (2020).

[23] A. Olacel, M. Boromiza, et al., Phys. Rev. C 106, 024609 (2022).
[24] G. Henning et al., in Proceedings of the 2015 4th International Conference on Advancements in Nuclear Instrumentation Measurement Methods and their Applications (ANIMMA), 2015, pp. 1-9, doi: 10.1109/ANIMMA.2015.7465505.
[25] M. Kerveno, et al., in Proceedings of the 15th International Conference on Nuclear Data for Science and Technology (ND2022).
[26] M.Kerveno et al., Physical Review C 87, 24609 (2013).
[27] M. Kerveno, et al., Phys. Rev. C 104, 044605 (2021).
[28] E. Party, PhD Thesis University of Strasbourg, paper in preparation.
[29] G. Henning et al., Proceedings of PHYSOR 2020 conference: https://hal.archives-ouvertes.fr/hal-02956052.
[30] W. Mondelaers and P. Schillebeeckx, Notiziario neutroni e luci di sincroton, 11, 19-25 (2010).
[31] L.C. Mihailescu, PhD Thesis, University of Bucharest (2006).
[32] L. C. Mihailescu, C. Borcea, and A. J. M. Plompen, Nucl. Instrum. Meth. Phys. Research A578, 298 (2007).
[33] https://www.struck.de/sis3316.html
[34] A.D. Carlson, et al., Nucl. Data Sheets 110, 3215 (2009).
[35] A. Plompen, et al., J. Korean Phys. Soc. 59, 1581 (2011).
[36] A. Olacel, PhD thesis, University of Bucharest (2015).
[37] M. Boromiza, PhD Thesis, University of Bucharest (2018).
[38] A. D. Carlson, V. G. Pronyaev, F.-J. Hambsch, W. Mannhart, A. Mengoni, R. O. Nelson, P. Talou, S. Tagesen, and H. Vonach, J. Korean Phys. Soc. 59, 1390 (2011).
[39] A. J. Koning, S. Hilaire, and M. C. Duijvestijn, in Proceedings of International Conference on Nuclear Data for Science and Technology, edited by O. Bersillon, F. Gunsing, E. Bauge, R. Jacqmin, and S. Leray, Nice, France (EDP Sciences, 2007), p. 211.
[40] T. von Egidy and D. Bucurescu, Phys. Rev. C 72, 044311 (2005).
[41] T. von Egidy and D. Bucurescu, J. Phys.: Conf. Ser. 338, 012028 (2012).
[42] Z. G. Ge, Z. X. Zhao, H. H. Xia, Y. X. Zhuang, T. J. Liu, J. S. Zhang, and H. C. Wu, J. Kor. Phys. Soc. 59, 1052 (2011).
[43] A. Lane, Nucl. Phys. 35, 676 (1962).
[44] A. Lane, Phys. Rev. Lett. 8, 171 (1962).
[45] A. Negret et al., Phys. Rev. C 88, 034604 (2013).
[46] J. E. Escher, J. T. Harke, F. S. Dietrich, N. D. Scielzo, I. J. Thompson, and W. Younes, Rev. Mod. Phys. 84, 353 (2012).
[47] C. Plettner et al., Phys. Rev. C 71, 051602(R) (2005).
[48] J. T. Burke et al., Phys. Rev. C 73, 054604 (2006).
[49] B. L. Goldblum, S. G. Prussin, U. Agvaanluvsan, L. A. Bernstein, D. L. Bleuel, W. Younes, and M. Guttormsen, Phys. Rev. C 78, 064606 (2008).
[50] M. Petit et al., Nucl. Phys. A 735, 345 (2004).
[51] S. Boyer et al., Nucl. Phys. A 775, 175 (2006).
[52] J. M. Allmond et al., Phys. Rev. C 79, 054610 (2009).
[53] S. Chiba and O. Iwamoto, Phys. Rev. C 81, 044604 (2010).
[54] A. Bohr and B. Mottelson, Nuclear Structure (World Scientific, Singapore, 1998).
[55] W. Hauser and H. Feshbach, Phys. Rev. 87, 366 (1952).
[56] A. Negret, et al., in Proceedings of the 15th International Conference on Nuclear Data for Science and Technology (ND2022).